Traffic 2000 **1**: 952–962
Munksgaard International Publishers

ISSN 1398-9219

Cholesterol is Required for the Formation of Regulated and Constitutive Secretory Vesicles from the *trans*-Golgi Network

Yanzhuang Wang, Christoph Thiele and Wieland B. Huttner*

Department of Neurobiology, Interdisciplinary Center of Neurosciences, University of Heidelberg, Im Neuenheimer Feld 364, 69120 Heidelberg, Germany, and Max-Planck-Institute of Molecular Cell Biology and Genetics, Pfotenhauerstrasse 110, D-01307 Dresden, Germany
** Corresponding author: W.B. Huttner, whuttner@sun0.urz.uni-heidelberg.de*

We studied the role of cholesterol in regulated protein secretion in neuroendocrine cells by manipulating the cholesterol content of AtT-20 cells. Depletion of cellular cholesterol levels caused a reversible block of immature secretory granule biogenesis at the level of the *trans*-Golgi-network, whereas increased cholesterol levels promoted immature secretory granule formation. Cholesterol depletion also blocked the formation of constitutive secretory vesicles, but did not inhibit the transport between the endoplasmic reticulum and the Golgi complex. Our results indicate that the assembly of cholesterol-based lipid microdomains is required for the biogenesis of both regulated and constitutive secretory vesicles from the *trans*-Golgi-network in neuroendocrine cells.

Key words: Cholesterol, *trans*-Golgi network, secretory vesicles, membrane curvature, lipid rafts

Received 28 August 2000, revised and accepted for publication 29 September 2000

Protein secretion is a common feature of virtually all eukaryotic cells. Certain cells such as neurons, endocrine and exocrine cells secrete proteins not only via the ubiquitous constitutive pathway, but also in a stimulus-dependent manner via the regulated pathway (1). Regulated secretory proteins (RSPs), destined to the regulated pathway, are packaged at the *trans*-Golgi network (TGN) into immature secretory granules (ISGs), which mature to the secretory granules, the organelles mediating regulated protein secretion (2–6).

The assembly of ISGs involves several steps – cargo segregation, cargo-membrane recognition and selection of certain integral membrane constituents into the nascent secretory granule membrane – all of which are only partially understood. The segregation of regulated from constitutive secretory proteins is accomplished by the selective aggregation of regulated secretory proteins in the TGN; this process is induced by the lumenal milieu of the TGN (7) and continues during maturation of ISGs (3,8). Recognition between the secretory cargo and membrane constituents that enter the forming ISG is thought to involve specific structures on RSPs, often referred to as 'sorting signals'. Sorting signals have been identified for several RSPs (9–11), but their interaction partners and mechanism of action remain controversial (5,8,12).

The assembly of the ISG membrane also includes sorting processes. Analogous to the self-aggregation of the regulated secretory cargo, lateral self-organization of membrane constituents, induced by the phase separation of lipids that occurs in membranes rich in cholesterol and sphingolipids (13), has been proposed to contribute to the formation of ISGs (14). Such cholesterol-dependent organization of membranes into lipid rafts plays an important role in several pathways of membrane traffic, including polarized secretion (15,16) and endocytosis (17,18). In addition, a specific interaction between cholesterol and a transmembrane protein (synaptophysin) was suggested to be essential for the generation of synaptic vesicles at the plasma membrane (19).

As the formation of lipid rafts critically depends on cholesterol levels, raft-dependent membrane traffic pathways can be discriminated from raft-independent pathways by their sensitivity to experimental reductions of cellular cholesterol levels (15). In this study, we show that the biogenesis of secretory vesicles from the TGN, and RSP packaging into immature secretory granules, critically depend on the cellular cholesterol level. Cholesterol effects on the traffic of RSPs are reversible and act specifically at the level of the TGN.

Results

Cholesterol depletion reversibly inhibits the formation of secretory vesicles from the TGN

We examined the consequences of altering cellular cholesterol levels on secretory granule biogenesis in the neuroendocrine cell line AtT-20. AtT-20 cells were grown in cholesterol-free medium in the presence of the inhibitor of endogenous cholesterol synthesis, Lovastatin (20), followed by analysis of the endogenous RSP pro-opiomelanocoertin (POMC). After 35 h of treatment with 10 μM Lovastatin, the cholesterol level relative to that of the phospholipids PC and PE was reduced to 50% of the control value, i.e. the cholesterol level of AtT-20 cells grown in medium supplemented with 15% delipidated serum (Table 1). Double immuno-

[1] Joint first authors.
[2] Present address: Department of Cell Biology, SHM C432, Yale University School of Medicine, 333 Cedar St., P.O. Box 208002, New Haven, CT 06520, USA.

fluorescence confocal microscopy showed that in AtT-20 cells grown in either normal growth medium supplemented with non-delipidated serum (Figure 1, control) or medium supplemented with delipidated serum (data not shown), POMC immunoreactivity was observed in both secretory vesicles and the Golgi complex. The latter was identified by immunostaining for GLUMEN, a Golgi-resident 29 kDa transmembrane protein whose lumenal domain corresponds to NESP55 (21) and which is encoded by the XL2 exon of the XLαs gene (22) (Y. Wang, R. Kehlenbach, M.J. Hannah and W.B. Huttner, unpublished data). Lovastatin treatment for 35 h resulted in (i) the accumulation of POMC immunoreactivity in the Golgi complex and (ii) the disappearance of secretory vesicles immunoreactive for POMC and/or processing products derived therefrom (Figure 1, 35 h LS). This disappearance presumably reflected POMC secretion without concomitant replenishment of the secretory vesicle pool due to a block of secretory vesicle formation from the Golgi complex.

Two observations demonstrated that the block of secretory vesicle formation from the Golgi complex upon Lovastatin treatment, which blocks the synthesis of all mevalonate-derived lipids, was due to a decrease in the level of cellular cholesterol rather than another lipid. First, no effect of Lovastatin was seen in AtT-20 cells grown in non-delipidated medium (data not shown), suggesting that the relevant mevalonate-derived lipid was present in serum. Second, the observed accumulation of POMC in the Golgi complex was readily reversed by addition of 0.25 mM cholesterol (complexed to cyclodextrin) in the continued presence of Lovastatin, in parallel with a replenishment of the cellular cholesterol level (Table 1). Punctate immunoreactive structures in the vicinity of the Golgi complex, likely to represent newly formed secretory vesicles, were observed already 15 min after addition of cholesterol (data not shown). Two hours after addition of cholesterol, the subcellular pattern of POMC immunoreactivity was similar to that of control cells, i.e. with immunoreactivity being observed in both the Golgi complex and secretory vesicles (Figure 1; 37 h LS, 2 h CH). Four hours after addition of cholesterol (Figure 1; 39 h LS, 4 h CH), the Golgi complex was largely cleared of POMC immunoreactivity, which now was observed in secretory vesicles distributed throughout the cytoplasm and concentrated in the tips of the cellular processes where secretory granules are known to accumulate (23). Compared to control cells, less POMC immunoreactivity was retained in the Golgi complex after cholesterol readdition, suggesting that an elevated cellular cholesterol level might promote the packaging of secretory cargo at the TGN.

Table 1: Cholesterol levels of AtT-20 cells

Growth condition	Relative cholesterol content
35 h delipidated medium	142 ± 19
35 h delipidated medium + 10 μM Lovastatin	70 ± 12
37 h delipidated medium + 10 μM Lovastatin + 2.5 mg/ml cholesterol-cyclodextrin during last 2 h	149 ± 26

Cholesterol levels are expressed relative to the sum of phosphatidylcholine plus phosphatidylethanolamine, and are given as percentages of the cholesterol level of cells grown in complete medium (100). Data are the mean ± SD; n = 3.

Raising the cellular cholesterol level promotes packaging of chromogranin B into post-Golgi vesicles

We next examined the effects of manipulating cholesterol levels on the subcellular distribution of chromogranin B (CgB), an RSP found in a wide variety of endocrine cells and neurons (24). In AtT-20 cells grown in normal medium (i.e. in the presence of 15% non-delipidated serum), only some CgB immunoreactivity was found in punctate structures likely to be secretory granules, whereas the majority of CgB colocalized with the Golgi complex (Figure 2, control). The fact that the CgB-containing vesicle population appears to be smaller than the one containing POMC at least partially reflects a higher sorting efficiency of CgB relative to POMC. Incubation of AtT-20 cells in the presence of cycloheximide (to prevent replenishing the Golgi pool of CgB) resulted in the clearance of CgB from the Golgi complex into secretory vesicles (data not shown), demonstrating the transient nature of the accumulation of CgB in the Golgi complex. We explored the possibility that this transient accumulation was due to limiting levels of cholesterol, i.e. that addition of cholesterol might increase the packaging of CgB into TGN-derived vesicles. While little change in the subcellular distribution of CgB was observed 1 h after addition of 0.25 mM cholesterol (complexed to cyclodextrin) (Figure 2, 1 h), 2 h after cholesterol addition, the Golgi localization of CgB was shifted to an almost completely vesicular localization (Figure 2, 2 h), which often was concentrated in the tips of the cellular processes (data not shown). We conclude that efficient formation of secretory granules containing CgB strongly depends on an adequate cellular cholesterol level and that the AtT-20 cells under the present growth conditions did not reach this level.

We used electron microscopy to determine at which level within the Golgi complex secretory protein traffic was affected by cholesterol depletion. AtT-20 cells treated with Lovastatin in delipidated medium for 35 h (Figure 3C + C′) showed a marked vacuolation of the TGN compared to control cells (Figure 3A + A′, Table 2), whereas the cisternae at the *cis*-face of the Golgi complex were unaffected. Frequently, the TGN vacuoles were found to contain electron-dense material, presumably condensed regulated secretory cargo, which usually was in contact with the membrane (Figure 3D + C′, asterisks). In the periphery of the cell, secretory granules were found to accumulate in control cells (Figure 3B) but not in cholesterol-depleted cells (not shown), consistent with the lack of peripheral immunoreactive puncta in immunofluorescence (compare Figure 1). The major morphological changes observed upon cholesterol depletion, i.e.

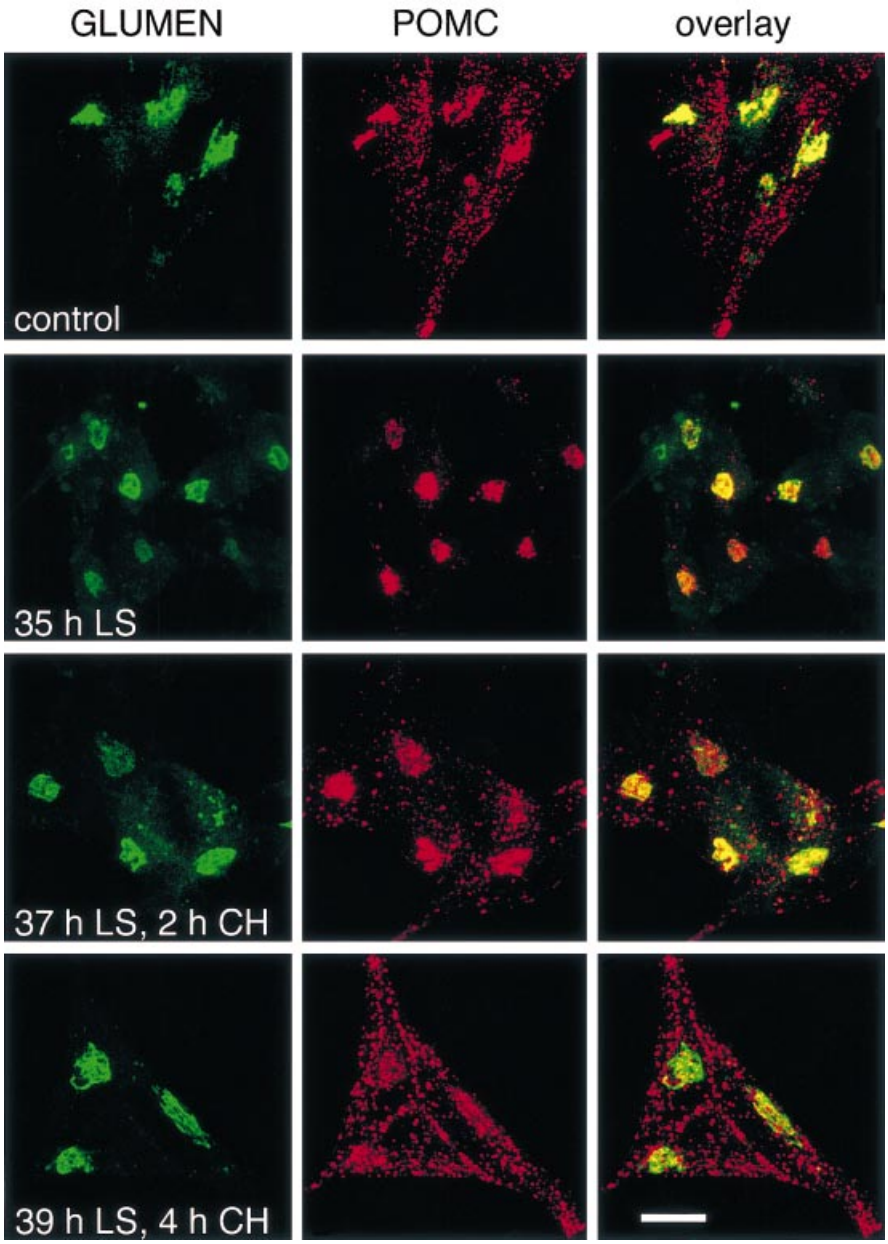

Figure 1: Cholesterol levels control the exit of POMC from the Golgi complex. Double immunofluorescence of AtT-20 cells grown (i) in normal growth medium (control), (ii) for 35 h in delipidated medium containing 10 μM Lovastatin (35 h LS), (iii, iv) for 35 h in delipidated medium containing 10 μM Lovastatin followed by addition of 5 mg/ml cholesterol-cyclodextrin complex and further incubation for (iii) 2 h (37 h LS, 2 h CH) or (iv) 4 h (39 h LS, 4 h CH). After fixation, cells were immunostained for the Golgi marker GLUMEN (green) and POMC (red). The pictures shown are composites of nine confocal sections encompassing the entire thickness of the cells to ensure that the Golgi complex and secretory vesicles, which are found in different horizontal planes, are equally represented in the pictures. Scale bar: 10 μm.

the vacuolation of the TGN and lack of peripheral secretory granules, were found to be reversible upon treatment of cholesterol-depleted cells with cholesterol (complexed to cyclodextrin). Figure 3E and E′ and Table 2 show the lack of vacuolated TGN in a cell replenished with cholesterol for 2 h; the accumulation of secretory granules in the periphery of a cholesterol-replenished cell is shown in Figure 3F. These observations suggested that the block of RSP traffic upon cholesterol depletion occurred at the level of the TGN.

Cholesterol depletion does not inhibit membrane traffic between the ER and the Golgi complex

As was the case in control cells (Figure 3A, small arrowheads), numerous small vesicles associated with the Golgi complex were observed in Lovastatin-treated cells (Figure 3C, small arrowheads). These vesicles presumably are the carriers mediating transport between Golgi cisternae and between the ER and the Golgi complex, implying that cholesterol depletion resulted in a specific block of secretory vesi-

cle formation from the TGN rather than a general defect in vesicular transport. To investigate this directly, we used the drug brefeldin A, which is known to cause the retrograde traffic to the ER of membrane constituents of the *cis*-, *medial*- and *trans*-Golgi, but not the TGN (25,26). Double immunofluorescence of Lovastatin-treated AtT-20 cells indicated that upon treatment for 30 min with brefeldin A in the continued presence of Lovastatin (Figure 4, BFA), the Golgi membrane marker GLUMEN became diffusely distributed throughout the cytoplasm, indicative of its redistribution to the ER. In contrast, POMC immunoreactivity remained in a clustered perinuclear location in a pattern very similar to that observed for Lovastatin-treated cells not exposed to brefeldin A (Figure 4, control). Three hours after wash-out of brefeldin A in the continued presence of Lovastatin, GLUMEN was again found in the typical location of the Golgi complex, apparently colocalized with POMC (Figure 4, wash-out). Both the diffuse redistribution of GLUMEN upon brefeldin A treatment as well as its reclustering in the perinuclear region upon brefeldin A wash-out were indistinguishable between Lovastatin-treated and untreated AtT-20 cells (data not shown). These observations demonstrate that both retrograde and anterograde membrane traffic between the Golgi complex and the ER still operate in cholesterol-depleted cells. Hence, the block of secretory vesicle formation upon cholesterol depletion reflects a specific effect on the TGN rather than on the entire ER–Golgi complex system.

Cholesterol is essential for the formation of both constitutive and regulated secretory vesicles from the TGN

To corrobarate these morphological findings with biochemical evidence, we used [^{35}S]sulfate pulse-chase labeling followed by subcellular fractionation (27) to investigate the effects of cholesterol depletion on secretory vesicle formation from the TGN. Control cells (grown in delipidated medium in the absence of Lovastatin) were pulse-labeled with [^{35}S]sulfate for 5 min and the postnuclear supernatant (PNS) was analyzed by velocity sucrose gradient centrifugation for the distribution of the constitutive secretory protein

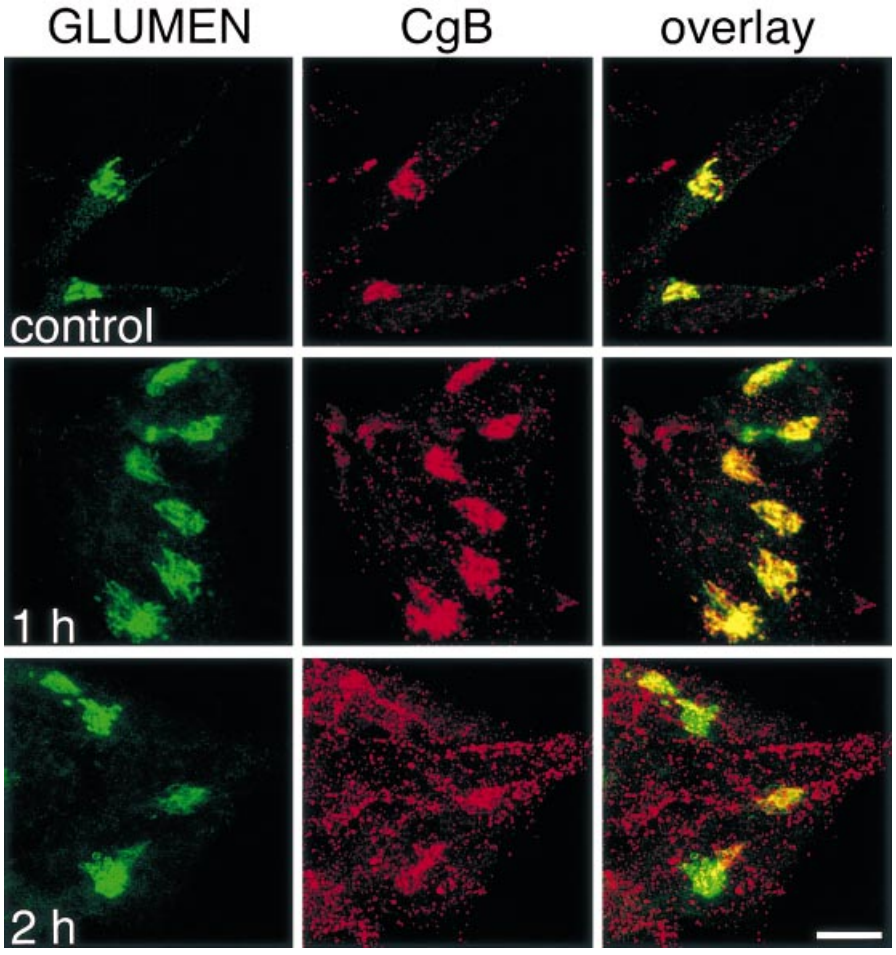

Figure 2: Addition of cholesterol promotes packaging of CgB into secretory granules. Double immunofluorescence of AtT-20 cells grown in normal growth medium (control) or in normal growth medium containing 10 mg/ml cholesterol-cyclodextrin complex for 1 h (1h) or 2 h (2h). After fixation, cells were immunostained for the Golgi marker GLUMEN (green) and CgB (red). The pictures shown are composites of nine confocal sections encompassing the entire thickness of the cells. Scale bar: 10 μm.

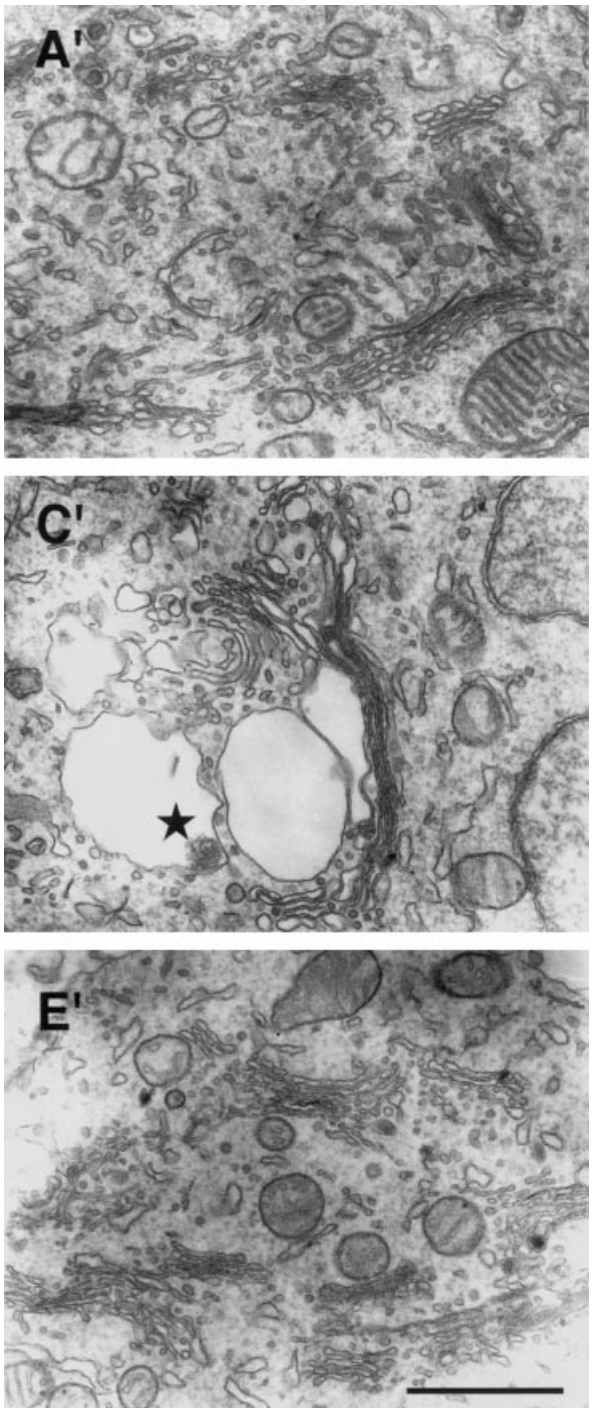

Figure 3: Cholesterol depletion induces reversible swelling and accumulation of condensed secretory cargo in, *trans*-Golgi cisternae. Electron microscopy of AtT-20 cells grown (i) in normal growth medium (A, A′ and B), (ii) for 35 h in delipidated medium containing 10 μM Lovastatin (C, C′ and D), and (iii) for 35 h in delipidated medium containing 10 μM Lovastatin followed by addition of 5 mg/ml cholesterol-cyclodextrin complex and further incubation for 2 h (E, E′ and F). Perinuclear regions containing the Golgi complex are shown in A, C and E. The *cis*- and *trans*-faces of the Golgi complex are labeled with c and t, respectively. Large arrowheads in A and E point to nascent immature secretory granules at the *trans*-face of the Golgi complex; small arrowheads in A, C and E point to smaller vesicles that are found close to the Golgi stack and are likely to mediate vesicular transport between Golgi cisternae. Note that *trans*-Golgi cisternae in cholesterol-depleted cells (C, C′) are significantly enlarged compared to both control cells (A, A′) and cholesterol-replenished cells (E, E′). Another *trans*-Golgi region of a cholesterol-depleted cell is shown in D; the enlarged cisternae contain condensed material (asterisks) in contact with the membrane, partially surrounded by a coat (small arrows). Sections through the periphery of the cell, containing large dense-core secretory granules, are shown in B and F. A′, C′, E′ show lower magnifications giving a better impression of overall changes in Golgi organization. Equal magnifications are shown in A, C and E; in A′, C′ and E′; and in B and F; bars represent 200 nm, the bar in E′ represents 1 μm.

p97 (28; 29) and POMC, which in AtT-20 cells is processed to the regulated secretory peptide ACTH. Consistent with previous observations (30), both sulfated p97 and sulfated POMC (as identified by immunoprecipitation; see Figure 5, top left panel) were found to peak in fractions 7 and 8, defining the position of the TGN in the gradient (Figure 5A). Upon a 15-min chase, the majority of both sulfated proteins were recovered in the upper half of the gradient, and POMC was partially proteolytically processed, with p97 peaking in fraction 2, POMC in fractions 2–4, and the sulfated ACTH-containing processing products of POMC in fractions 3 and 4 (Figure 5C). The differential distribution of p97 and the sulfated ACTH-containing processing products of POMC in the top fractions of the gradient indicated that two populations of TGN-derived secretory vesicles were formed, i.e. constitutive secretory vesicles and immature secretory granules. The

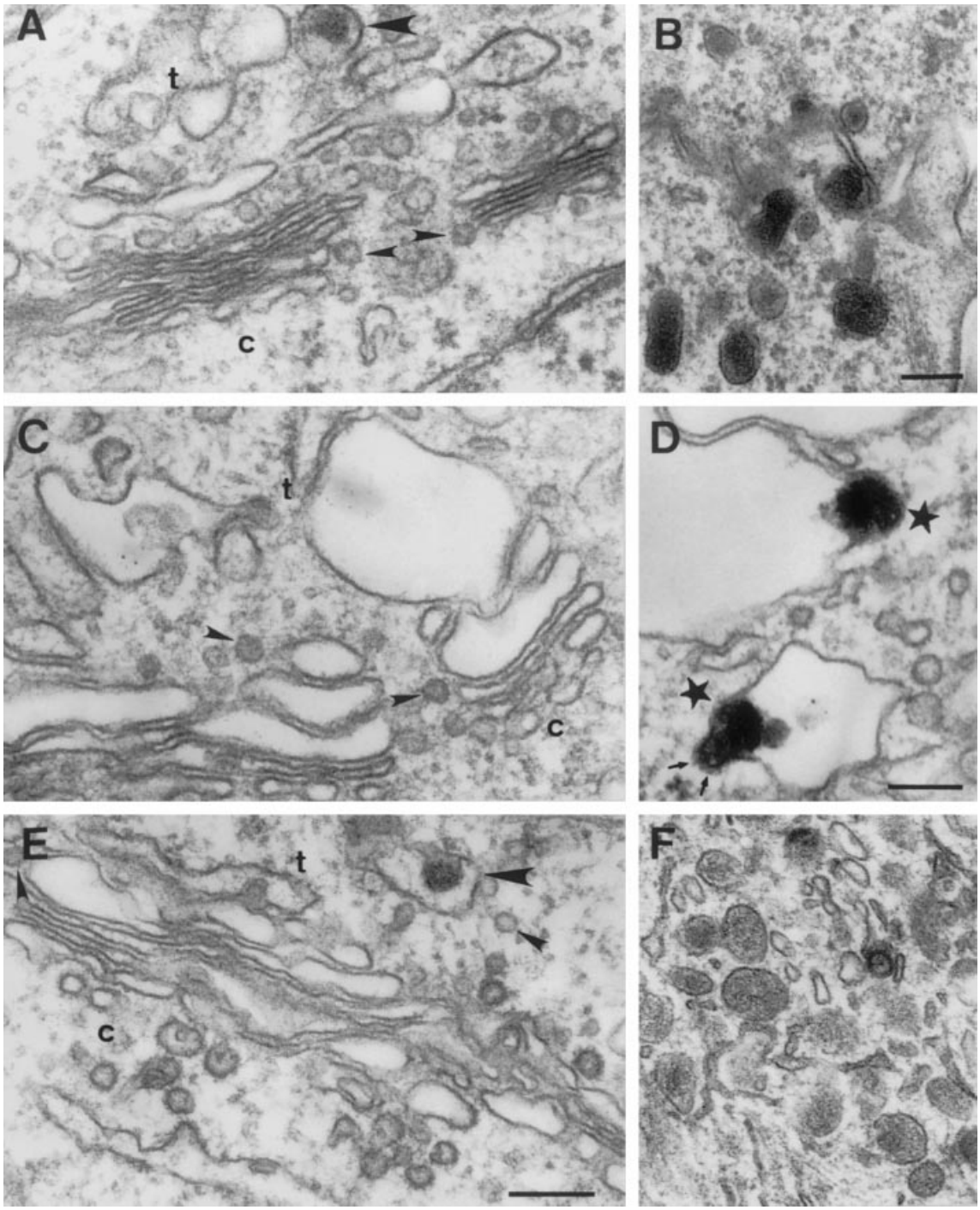

Figure 3:

observation that the peak of POMC comprised the peak of both p97 and the POMC processing products is consistent with previous observations that in AtT-20 cells, POMC exits from the TGN in both constitutive secretory vesicles and immature secretory granules but is processed only in the latter (28,29).

As was the case with control AtT-20 cells, in cells treated for 35 h with Lovastatin in delipidated medium, both p97 and POMC were found in the TGN position of the gradient after a 5 min [^{35}S]sulfate pulse (Figure 5B). However, both p97 and POMC remained in the TGN position of the gradient during a 15-min chase indicating that the formation of constitutive secretory vesicles and immature secretory granules was blocked in the Lovastatin-treated cells (Figure 5D). A small up-shift in the gradient of low molecular weight processing products probably does not reflect formation of

secretory vesicles but fragmentation of the TGN during cell homogenization. Consistent with the immunofluorescence observations (Figure 1), the inhibitory effect of Lovastatin on the formation of both types of vesicles was reversed by the addition of 0.13 mM cholesterol (in the continued presence of Lovastatin) to the medium 2.5 h before the pulse-chase

Table 2: Effects of cholesterol removal and replenishment on the morphology of the AtT-20 Golgi complex

Growth condition	Cisternae per stack	Dilated *trans* cisternae per stack	TGN vacuoles per stack
Normal growth medium	5.3 ± 0.8	0.16 ± 0.4	n.d.
35 h delipidated medium + 10 μM Lovastatin	4.7 ± 0.8	2.3 ± 1.4	1.3 ± 1.0
37 h delipidated medium + 10 μM Lovastatin + 5 mg/ml cholesterol-cyclodextrin during last 2 h	4.7 ± 0.5	2.0 ± 1.4	n.d.

Profiles of Golgi stacks in electron micrographs obtained as in Figure 3 were analyzed for the total number of cisternae per stack, the number of dilated cisternae at the *trans* side of the stack, and the number of TGN vacuoles adjacent to the stack. The *trans* side of the stack and the TGN were identified by the presence of condensed secretory cargo. For each condition, six Golgi stacks of different cells were quantitated. Data are the mean ± SD; n.d., not detectable.

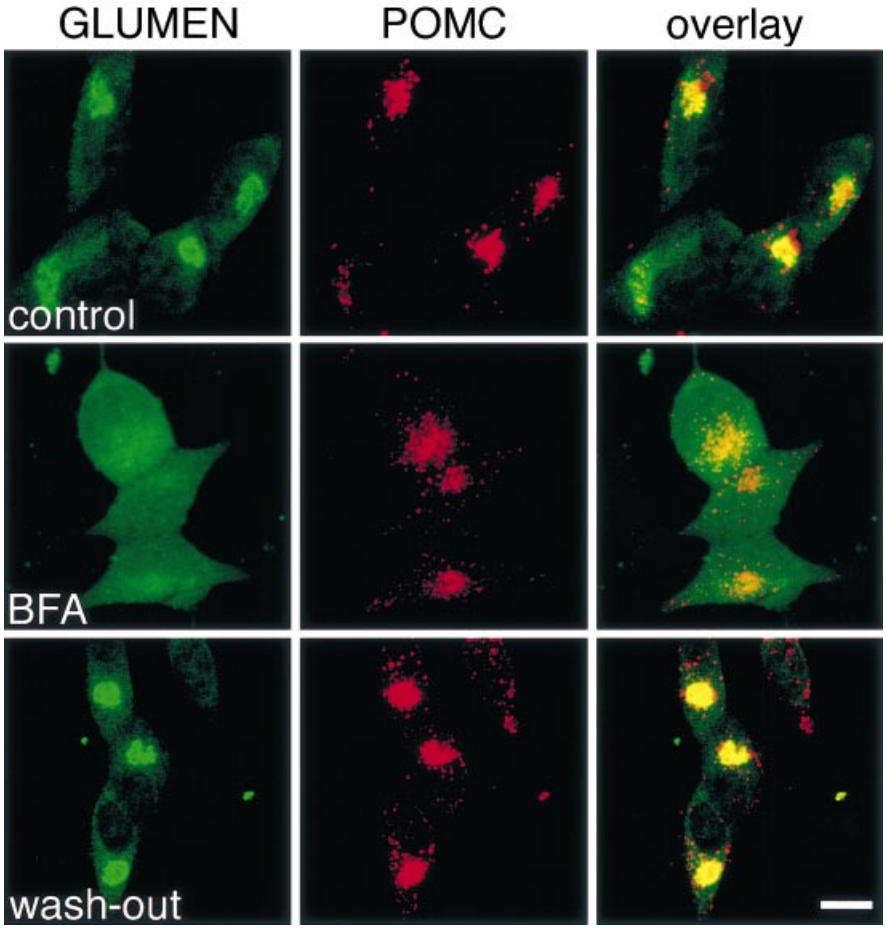

Figure 4: Cholesterol depletion does not block anterograde and retrograde membrane traffic between the ER and the Golgi complex. Double immunofluorescence of AtT-20 cells grown in delipidated medium containing 10 μM Lovastatin either for 36 h (control), for 36 h followed by 0.5 h in the presence of 2.5 μg/ml brefeldin A (BFA), or for 36 h followed by 0.5 h in the presence of 2.5 μg/ml brefeldin A followed by 3 h in the absence of brefeldin A (wash-out). After fixation, cells were immunostained for the Golgi marker GLUMEN (green) and POMC (red). The pictures shown are composites of nine confocal sections encompassing the entire thickness of the cells. Scale bar: 10 μm.

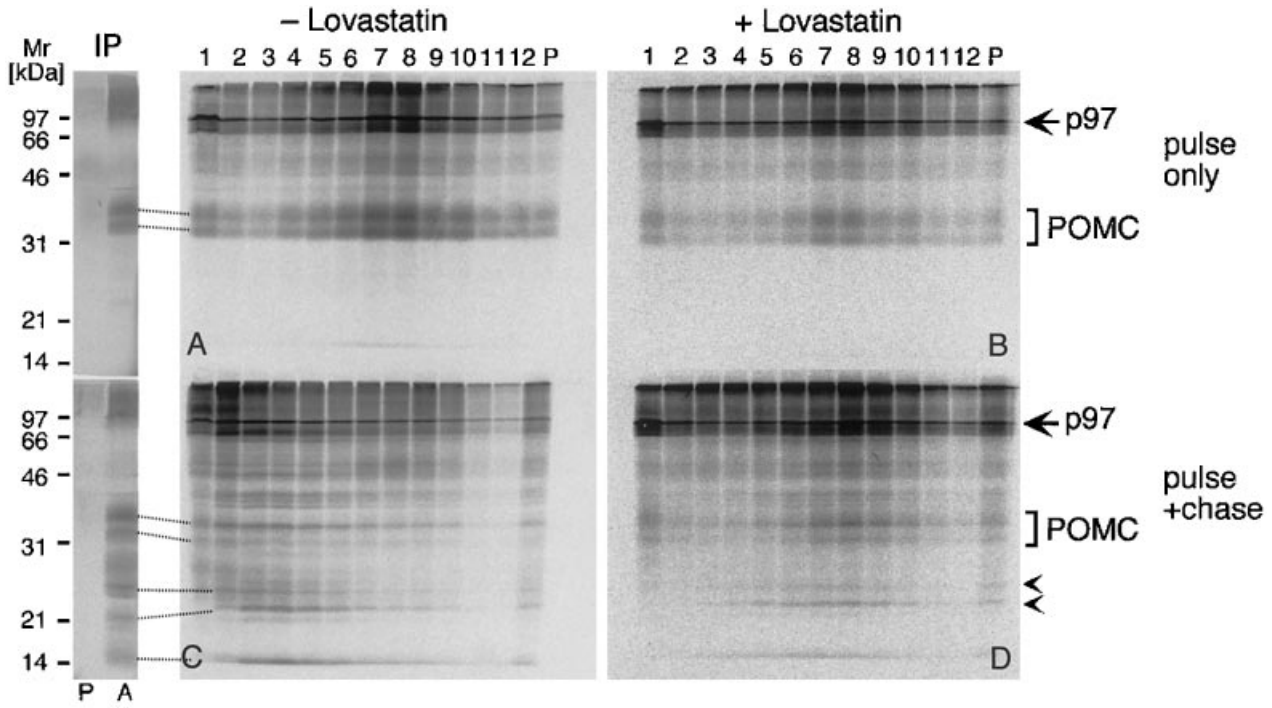

Figure 5: Cholesterol depletion blocks formation of secretory vesicles from the TGN. AtT-20 cells were grown for 36 h in delipidated medium and pulse-labeled in delipidated medium with reduced serum content for 5 min with [^{35}S]sulfate (A, B) followed by chase for 15 min (C, D), all in the absence (left panels) or presence (right panels) of 10 μM Lovastatin. (A–D) The PNS was subjected to velocity sucrose gradient centrifugation and the fractions were analyzed for [^{35}S]sulfate-labeled proteins by SDS-PAGE followed by phosphoimaging. The top fraction (fraction 1) is shown at the left, the pellet (P) at the right. Arrows indicate p97, a constitutively secreted protein, and brackets POMC. The TGN, as defined by the [^{35}S]sulfate pulse, peaks in fractions 7 and 8; constitutive secretory vesicles, as defined by the position of [^{35}S]sulfate-labeled p97 after the 15 min chase, peak in fraction 2; immature secretory granules, as defined by the position of [^{35}S]sulfate-labeled POMC processing products (arrowheads) after the 15 min chase, peak in factions 3 and 4. The two lanes to the left of panels A and C show the immunoprecipitates (IP) from the PNS obtained with preimmune serum (P) and anti-ACTH antiserum (A). The dotted lines indicate the corresponding bands of POMC and POMC-derived processing products.

experiment (data not shown). No block of TGN-derived vesicle formation by Lovastatin was observed in cells grown in normal medium (data not shown).

Discussion

We have shown that cholesterol is an essential component for secretory granule formation from the TGN, with cholesterol addition promoting and cholesterol depletion inhibiting this process. The inhibitory effect of cholesterol depletion is not confined to the regulated pathway of secretion but also concerns the formation of constitutive secretory vesicles in neuroendocrine cells, consistent with previous observations on the apical transport vesicle in MDCK cells (15) and the axonal transport vesicle in neurons (16). However, cholesterol depletion does not inhibit membrane traffic more proximal in the secretory pathway since neither the retrograde transport from the Golgi complex to the ER in the presence of brefeldin A nor the anterograde ER-to-Golgi transport upon brefeldin A wash-out was blocked in cholesterol-depleted cells. Similarly, biosynthetic ER-to-Golgi transport in MDCK cells has been found to be unaffected by cholesterol depletion (15). Hence, cholesterol depletion does not perturb vesicular transport from, and to, the Golgi complex in an unspecific manner, but selectively blocks secretory vesicle formation from the TGN.

Which step of secretory vesicle biogenesis is inhibited by cholesterol depletion? As revealed by electron microscopy, ISG buds at the TGN containing aggregated/condensed secretory cargo and partial clathrin coats were frequently present in cholesterol-depleted cells. Hence, cholesterol depletion does not perturb lumenal parameters required for aggregation/condensation, notably TGN acidification (31,32), and allows the initiation of the budding process. However, ISG buds ready to pinch-off from the TGN were not observed. This suggests that cholesterol depletion blocks the last steps of the budding process and the fission step. These steps are characterized by the generation of negative curvature in the lumenal membrane leaflet. It is interesting to note that the formation of endocytic vesicles from the plasma membrane is also arrested upon cholesterol depletion at the transition from shallow to deeply invaginated clathrin-coated pits (17,18).

Why would cholesterol depletion interfere with the generation of negative membrane curvature in the lumenal leaflet of secretory vesicles budding from the TGN? A feature that distinguishes such vesicles from those more proximal in the secretory pathway is their higher contents of glycosphingolipids (e.g. the ganglioside GM3 in secretory granules (33)), whose synthesis is completed in the TGN and which are confined to the lumenal membrane leaflet (34). Glycosphingolipids are characterized by bulky polar headgroups, saturated fatty acyl chains and the *trans*-unsaturated sphingosine, all of which contribute to an inverted-cone shape that is better compatible with positive than negative membrane curvature. We propose that in order to be incorporated into the lumenal leaflet of secretory vesicles, glycosphingolipids need to interact with cone-shaped lipids that favor negative membrane curvature. Cholesterol is such a lipid (35).

Cholesterol and glycosphingolipids are the key components of lipid rafts (13,36). A characteristic feature of lipid rafts is their insolubility in certain detergents such as Triton X-100 (37). The membrane of secretory granules, like the membranes of constitutive secretory vesicles (15), contain detergent-insoluble complexes (38) that float in density gradients and hence can be considered lipid rafts (19). Our observation that cholesterol is essential for the biogenesis of secretory vesicles from the TGN therefore suggests that this process requires the formation of lipid rafts. In other words, assembly of glycosphingolipids together with cholesterol into lipid rafts may be a means of packaging glycosphingolipids into the negatively curved lumenal leaflet of secretory vesicles. In this context, it should be noticed that the cholesterol requirement for both the generation of vesicle curvature and lipid raft assembly might also be differential for the various types of vesicles formed at the TGN, with lipid raft assembly being more important for one vesicle type and curvature generation for the other.

The proposal that assembly of cholesterol-based lipid rafts overcomes the lack-of-negative-curvature problem intrinsic to glycosphingolipids is consistent with several observations. First, glycolipids are preferentially delivered to the apical surface of polarized epithelial cells (39), and the apical secretory pathway is more sensitive to cholesterol depletion than the basolateral pathway (15). Second, synaptic vesicles contain very low levels of glycosphingolipids, in contrast to the presynaptic plasma membrane from which they originate (40). In fact, given that synaptic vesicles are the smallest membrane vesicles known, both the exclusion of glycosphingolipids during, and the cholesterol dependence of, their biogenesis (19) may reflect the need of generating the extreme negative curvature of their lumenal membrane leaflet. Third, the lumenal leaflet of the secretory granule membrane contains a remarkably high concentration of lyso-phosphatidylcholine (41), which, although not a glycosphingolipid, nonetheless is an inverted-cone-shaped lipid that, alone, would induce positive membrane curvature. Interestingly, lyso-phosphatidylcholine, like glycosphingolipids, forms complexes with cholesterol (42,43).

As a corollary to this, one would expect that the coalescence of lipid rafts within the TGN membrane segment that forms the future vesicle should coincide with secretory vesicle formation. Indeed, this is precisely what has been observed in the case of apical constitutive secretory vesicles (44). It is interesting to note that none of the coats mediating the formation of vesicles in the early secretory system (COPI and COPII) (45–47) and in the endocytic pathway (clathrin) (48) appear to be involved in secretory vesicle formation from the TGN. (The partial clathrin coats found on ISGs are thought to play a role in ISG maturation rather than ISG formation from the TGN (5,6).) Perhaps the coalescence of lipid rafts, i.e. a phase separation occurring in the TGN membrane, contributes to the driving force for the formation of secretory vesicles, parallel to the aggregation of secretory cargo in the lumen of the nascent ISG (14).

Materials and Methods

AtT-20 cell culture

AtT-20 cells were grown in DMEM supplemented with 12.5% horse serum and 2.5% fetal calf serum in a 5% CO_2 atmosphere. If indicated, sera were delipidated by solvent extraction as follows. Serum was mixed with an equal volume of a 2:1 mixture of diisopropyl ether: n-butanol, stirred at room temperature for 30 min, and phases were separated by centrifugation at $5000 \times g$ for 30 min. The aqueous phase was re-extracted as above except that only diisopropyl ether was used, and extensively dialyzed against PBS. This treatment resulted in the reduction of the cholesterol content to $< 5\%$ of untreated serum, as determined using a colorimetric assay kit (Boehringer-Mannheim, Indianapolis, IN). In some experiments, AtT-20 cells were grown in the presence of Lovastatin (a kind gift of Merck, Sharp and Dome, Munich, Germany) as indicated. Cholesterol complexed to methyl-β-cyclodextrin (from Sigma, St. Louis, MO) was prepared as described (49). Cholesterol complexed to methyl-β-cyclodextrin was added to cells without and with prior Lovastatin treatment; in the latter case, the presence of Lovastatin was continued.

Pulse-chase labeling of AtT-20 cells followed by subcellular fractionation

Pulse-chase labeling of AtT-20 cells was performed following established protocols (27,30). Briefly, AtT-20 cells were grown to 50% confluency in normal growth medium. The medium was replaced by DMEM supplemented with delipidated sera, without or with 10 μM Lovastatin, and the cells were grown for further 36 h. The cells were washed with labeling medium (sulfate-free DMEM supplemented with 6.25% delipidated horse serum and 1.25% delipidated fetal calf serum), equilibrated in 5 ml labeling medium for 5 min, and then pulse-labeled in this medium for 5 min by the addition of 5 mCi carrier-free [^{35}S]sulfate. When indicated, the cells were chased for 15 min in 10 ml labeling medium lacking [^{35}S]sulfate and containing 3.2 mM Na_2SO_4. Pulse-chase labeling of cells grown in the presence of Lovastatin was performed in the continued presence of 10 μM Lovastatin. The cells were harvested, a PNS was prepared and subjected to velocity sucrose gradient centrifugation (0.3–1.4 M sucrose) as described (27). The gradients were fractionated (12 fractions plus pellet) and [^{35}S]sulfate-labeled proteins were analyzed by SDS-PAGE followed by phosphoimaging. Immunoprecipitation of ACTH-containing peptides from the PNS of [^{35}S]sulfate-labeled AtT-20 cells was performed as described (29).

Double immunofluorescence confocal microscopy

Double immunofluorescence of paraformaldehyde-fixed AtT-20 cells on coverslips was performed according to standard procedures (50), using either mAb219.6 against rat CgB (50) or mAb1E4 (Biogenesis, Poole, UK) against the 50 N-terminal residues of human POMC and affinity-purified rabbit antibody against GLUMEN, a Golgi-resident 29 kDa transmembrane protein whose lumenal domain corresponds to NESP55 (21) and which is encoded by the XL2 exon of the rat XLαs gene (22) (Y. Wang, R. Kehlenbach, M.J. Hannah and W.B. Huttner, unpublished results). The immunostaining pattern for the latter protein was very similar to, if not indistinguishable from, that for the established Golgi marker GM130 (51) (data not shown). The primary antibodies were detected by LRSC-conjugated goat antibody against mouse IgG (Dianova, Hamburg, Germany) and FITC-conjugated goat antibody against rabbit IgG (ICN, Costa Mesa, CA). The coverslips were mounted in Moviol and observed with a Leica (Mannheim, Germany) TCS^{4D} confocal laser scanning microscope. The confocal microscope settings were such that the photomultipliers were within their linear range. The images shown were prepared from the confocal data files using Adobe (Mountain View, CA) photoshop software.

Electron microscopy

AtT-20 cells were washed with 100 mM cacodylate buffer pH 7.4, fixed with 1% glutaraldehyde in cacodylate buffer, postfixed in 1% (w/v) OsO_4/1.5% (w/v) magnesium ferricyanide, and contrasted with 1.5% (w/v) magnesium uranyl acetate. Samples were then dehydrated in ethanol and embedded in Epon. Ultrathin sections were contrasted with uranyl acetate and lead citrate and observed in a Zeiss EM 10 CR electron microscope.

Cholesterol and phospholipid determination

Aliquots of pelleted membranes were extracted with chloroform/methanol using a modified version of the Wessel-Fluegge protocol (52), and the lipids in the chloroform phase were separated by thin-layer chromatography using silica gel 60 (Merck, Darmstadt, Germany) and chloroform:methanol:water 65:25:4. Lipids were visualized by spraying the plate with 20% sulfuric acid followed by heating to 140°C. Cholesterol appeared as a red spot and phospholipids as yellow-green spots. The spots were scanned and quantified using the MacBas software package.

Acknowledgments

We thank Andrea Hellwig for performing the electron microscopy and Dr. Matthew Hannah for advice with confocal microscopy and for helpful comments on the manuscript. Y.W. was the recipient of fellowships from the State of Baden-Wuerttemberg and from the Graduiertenkolleg 'Molecular Cell Biology' of the Deutsche Forschungsgemeinschaft. W.B.H. was supported by grants from the DFG (SFB 317, C2), the EC (ERB-FMRX-CT96-0023 and ERB-BIO4CT960058), the German-Israeli Foundation for Scientific Research and Development, and the Fonds der Chemischen Industrie.

References

1. Burgess TL, Kelly RB. Constitutive and regulated secretion of proteins. Ann Rev Cell Biol 1987;3: 243–293.
2. Tooze SA, Flatmark T, Tooze J, Huttner WB. Characterization of the immature secretory granule, an intermediate in granule biogenesis. J Cell Biol 1991;115: 1491–1503.
3. Tooze SA, Chanat E, Tooze J, Huttner WB. Secretory granule formation. In Peng Loh Y (Ed.), Mechanisms of Intracellular Trafficking and Processing of Proproteins. Boca Raton: CRC Press, 1993: 157–177.
4. Halban PA, Irminger J-C. Sorting and processing of secretory proteins. Biochem J 1994;299: 1–18.
5. Arvan P, Castle D. Sorting and storage during secretory granule biogenesis: looking backward and looking forward. Biochem J 1998;332: 593–610.
6. Tooze SA. Biogenesis of secretory granules in the trans-Golgi network of neuroendocrine and endocrine cells. Biochim Biophys Acta 1998;1404: 231–244.
7. Chanat E, Huttner WB. Milieu-induced, selective aggregation of regulated secretory proteins in the *trans*-Golgi network. J Cell Biol 1991;115: 1505–1519.
8. Thiele C, Gerdes H-H, Huttner WB. Puzzling receptors. Curr Biol 1997;7: R496–R500.
9. Chanat E, Weiß U, Huttner WB, Tooze SA. Reduction of the disulfide bond of chromogranin B (secretogranin I) in the *trans*-Golgi network causes its missorting to the constitutive secretory pathway. EMBO J 1993;12: 2159–2168.
10. Cool DR, Normant E, Shen F-S, Chen H-C, Pannell L, Zhang Y, Loh YP. Carboxypeptidase E is a regulated secretory pathway sorting receptor: genetic obliteration leads to endocrine disorders in Cpe^{fat} mice. Cell 1997;88: 73–83.
11. Kroemer A, Glombik MM, Huttner WB, Gerdes H-H. Essential role of the disulfide-bonded loop of chromogranin B for sorting to secretory granules is revealed by expression of a deletion mutant in the absence of endogenous granin synthesis. J Cell Biol 1998;140: 1331–1346.
12. Irminger J-C, Verchere CB, Meyer K, Halban PA. Proinsulin targeting to the regulated pathway is not impaired in carboxypeptidase E-deficient Cpe^{fat}/Cpe^{fat} mice. J Biol Chem 1997;272: 27532–27534.
13. Simons K, Ikonen E. Functional rafts in cell membranes. Nature 1997;387: 569–572.
14. Thiele C, Huttner WB. Protein and lipid sorting from the *trans*-Golgi network to secretory granules-recent developments. Sem Cell Dev Biol 1998;9: 511–516.
15. Keller P, Simons K. Cholesterol is required for surface transport of influenza virus hemagglutinin. J Cell Biol 1998;140: 1357–1367.
16. Ledesma MD, Simons K, Dotti CG. Neuronal polarity: essential role of protein-lipid complexes in axonal sorting. Proc Natl Acad Sci USA 1998;95: 3966–3971.
17. Rodal SK, Skretting G, Garred O, Vilhardt F, van Deurs B, Sandvig K. Extraction of cholesterol with methyl-β-cyclodextrin perturbs formation of clathrin-coated endocytic vesicles. Mol Biol Cell 1999;10: 961–974.
18. Subtil AIG, Kobylarz K, Lampson MA, Keen JH, McGraw TE. Acute cholesterol depletion inhibits clathrin-coated pit budding. Proc Natl Acad Sci USA 1999;96: 6775–6780.
19. Thiele C, Hannah MJ, Fahrenholz F, Huttner WB. Cholesterol binds to synaptophysin and is required for biogenesis of synaptic vesicles. Nat Cell Biol 2000;2: 42–49.
20. Alberts A. Discovery, biochemistry and biology of lovastatin. Am J Cardiol 1988;62: 10J–15J.
21. Ischia R, Lovisetti-Scamihorn P, Hogue-Angeletti R, Wolkersdorfer M, Winkler H, Fischer-Colbrie R. Molecular cloning and characterization of NESP55, a novel chromogranin-like precursor of a peptide with 5-HT1B receptor antagonist activity. J Biol Chem 1997;272: 11657–11662.
22. Kehlenbach RH, Matthey J, Huttner WB. XLαs is a new type of G protein. Nature 1994;372: 804–809.
23. Rivas RJ, Moore HP. Spatial segregation of the regulated and constitutive secretory pathways. J Cell Biol 1989;109: 51–60.

24. Huttner WB, Gerdes H-H, Rosa P. The granin (chromogranin/secretogranin) family. Trends Biochem Sci 1991;16: 27–30.
25. Lippincott-Schwartz J, Yuan L, Tipper C, Amherdt M, Orci L, Klausner RD. Brefeldin A's effects on endosomes, lysosomes, and the TGN suggest a general mechanism for regulating organelle structure and membrane traffic. Cell 1991;67: 601–616.
26. Rosa P, Barr FA, Stinchcombe JC, Binacchi C, Huttner WB. Brefeldin A inhibits the formation of constitutive secretory vesicles and immature secretory granules from the *trans*-Golgi network. Eur J Cell Biol 1992;59: 265–274.
27. Tooze SA, Huttner WB. Cell-free protein sorting to the regulated and constitutive secretory pathways. Cell 1990;60: 837–847.
28. Moore H-P, Gumbiner B, Kelly RB. A subclass of proteins and sulfated macromolecules secreted by AtT20 (mouse pituitary tumor) cells is sorted with adrenocorticotropin into dense secretory granules. J Cell Biol 1983;97: 810–817.
29. Natori S, Huttner WB. Chromogranin B (secretogranin I) promotes sorting to the regulated secretory pathway of processing intermediates derived from a peptide hormone precursor. Proc Natl Acad 1996;93: 4431–4436.
30. Fernandez CJ, Haugwitz M, Eaton B, Moore H-PH. Distinct molecular events during secretory granule biogenesis revealed by sensitivities to brefeldin A. Mol Biol Cell 1997;8: 2171–2185.
31. Gerdes H-H, Rosa P, Phillips E, Baeuerle PA, Frank R, Argos P, Huttner WB. The primary structure of human secretogranin II, a widespread tyrosine-sulfated secretory granule protein that exhibits low pH- and calcium-induced aggregation. J Biol Chem 1989;264: 12009–12015.
32. Chanat E, Pimplikar SW, Stinchcombe JC, Huttner WB. What the granins tell us about the formation of secretory granules in neuroendocrine cells. Cell Biophysics 1991;19: 85–91.
33. Geissler D, Martinek A, Margolis RU, Margolis RK, Skrivanek JA, Ledeen R, Konig P, Winkler H. Composition and biogenesis of complex carbohydrates of ox adrenal chromaffin granules. Neuroscience 1977;2: 685–693.
34. van Meer G, Holthuis J. Sphingolipid transport in eukaryotic cells. Biochim Biophys Acta 2000;1486: 145–170.
35. Chen Z, Rand R. The influence of cholesterol on phospholipid membrane curvature and bending elasticity. Biophys J 1997;73: 267–276.
36. Brown D, London E. Functions of lipid rafts in biological membranes. Annu Rev Cell Dev Biol 1998;14: 111–136.
37. Brown DA, Rose JK. Sorting of GPI-Anchored proteins to glycolipid-enriched membrane subdomains during transport to the apical cell surface. Cell 1992;68: 533–544.
38. Pryde JG, Phillips JH. Fractionation of membrane proteins by temperature-induced phase separation in Triton X-114. Biochem J 1986;233: 525–533.
39. van Meer G, Stelzer EHK, Wijnaendts-van-Resandt RW, Simons K. Sorting of sphingolipids in epithelial (Madin-Darby canine kidney) cells. J Cell Biol 1987;105: 1623–1635.
40. Breckenridge WC, Morgan IG, Zanetta JP, Vincendon G. Adult rat brain synaptic vesicles. II. Lipid composition. Biochim Biophys Acta 1973;320: 681–686.
41. Westhead EW. Lipid composition and orientation in secretory vesicles. Ann NY Acad Sci 1987;493: 92–100.
42. Chauhan V, Ramsammy L, Brockerhoff H. Molecular interactions in the hydrogen belts of membranes. Glucose 6 phosphatase, lysophosphatidylcholine and cholesterol. Biochim Biophys Acta 1984;772: 239–243.
43. Chatelain P, Brasseur R. A conformational analysis study of the interaction of amiodarone and cholesterol with lysophosphatidylcholine. Biochem Pharmacol 1991;41: 1639–1647.
44. Röper K, Corbeil D, Huttner WB. Retention of prominin in microvilli reveals distinct cholesterol-based lipid micro-domains in the apical plasma membrane. Nat Cell Biol 2000;2: 582–592.
45. Rothman JE. Mechanisms of intracellular protein transport. Nature 1994;372: 55–63.
46. Schekman R, Orci L. Coat proteins and vesicle budding. Science 1996;271: 1526–1533.
47. Nickel W, Bruegger B, Wieland FT. Protein and lipid sorting between the endoplasmatic reticulum and the Golgi complex. Sem Cell Dev Biol 1998;9: 493–502.
48. Schmid S. Clathrin-coated vesicle formation and protein sorting: an integrated process. Annu Rev Biochem 1997;66: 511–548.
49. Klein U, Gimpl G, Fahrenholz F. Alteration of the myometrial plasma membrane cholesterol content with beta cyclodextrin modulates the binding affinity of the oxytocin receptor. Biochemistry 1995;34: 13784–13793.
50. Rosa P, Weiss U, Pepperkok R, Ansorge W, Niehrs C, Stelzer EHK, Huttner WB. An antibody against secretogranin I (chromogranin B) is packaged into secretory granules. J Cell Biol 1989;109: 17–34.
51. Nakamura N, Rabouille C, Watson R, Nilsson T, Hui N, Slusarewicz P, Kreis TE, Warren G. Characterization of a *cis*-Golgi matrix protein, GM130. J Cell Biol 1995;131: 1715–1726.
52. Wessel D, Fluegge UI. A method for the quantitative recovery of protein in dilute solution in the presence of detergents and lipids. Anal Biochem 1984;138: 141–143.